Glaizer 2000 Langmuir


David J Vanderah
Institute for Bioscience and Biotechnology R…

Thomas B Parr
University of Delaware


Curtis W Meuse
National Institute of Standards and Technolo…

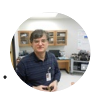
Gintaras Valincius
Vilnius University

Reconstitution of the Pore-Forming Toxin α-Hemolysin in Phospholipid/18-Octadecyl-1-thiahexa(ethylene oxide) and Phospholipid/*n*-Octadecanethiol Supported Bilayer Membranes

S. A. Glazier,[†] D. J. Vanderah,[†] A. L. Plant,[†] H. Bayley,[‡] G. Valincius,[†,§] and J. J. Kasianowicz*,[†]

National Institute of Standards and Technology, Biotechnology Division, Biomolecular Materials Group, Gaithersburg, Maryland 20899, The Texas A&M University System, Health Science Center, Department of Medical Genetics and Biochemistry, 440 Reynolds Building, College Station, Texas 77843-1114, and Department of Physical Chemistry, Vilnius University, Naugarduko 24, Vilnius 2006, Lithuania

Received May 19, 2000. In Final Form: October 11, 2000

We are studying the functional reconstitution of membrane-bound proteins into supported bilayer membranes (SBMs). Here, we describe the physical properties of SBMs formed by a layer of egg-phosphatidyl choline deposited on a monolayer of either 18-octadecyl-1-thiahexa(ethylene oxide) [THEO-C_{18}] or *n*-octadecanethiol on gold. We also show that the pore-forming protein α-hemolysin (αHL) self-assembles in these thin films. The insulating properties and the stability of the THEO-C_{18} self-assembled monolayers were characterized by ac impedance spectroscopy and voltammetry. An impedance model, including constant phase elements, was determined for THEO-C_{18} monolayers and the SBMs. Cyclic voltammetry measurements demonstrated virtually full blockage of ferricyanide oxidation and reduction by the THEO-C_{18} monolayers. The monolayer stability test showed that, at applied potentials between ±400 mV versus Ag/AgCl in 3 M KCl, the electrical properties of THEO-C_{18} SAMs did not change with time. The reconstitution of αHL in SBMs caused a decrease in impedance and an increased permeability to redox ions. The impedance model parameters suggest that αHL partially penetrates into the SBMs, increasing the dielectric constant of the alkane portion of the monolayers. The complete reconstitution of αHL that could provide the free access of the redox ions to the metal surface was not observed in these thin films.

Introduction

Supported bilayer membranes (SBMs) comprised of alkanethiol and phospholipid[1−8] have potential for applications requiring robust structures containing components such as membrane proteins. Simple alkanethiols do not provide an ideal matrix for transmembrane proteins because they form a hydrophobic monolayer that is attached directly to the solid support and therefore do not permit a hydrated region to exist at the substrate interface. Moreover, the monolayer is not in the fluid phase. A number of strategies for producing an aqueous environment on both sides of SBMs have been reported,[9−15] but none has been directly compared to SBMs formed from simple alkanethiols. Thus, in an effort to produce a SBM that simultaneously provides a suitable environment for the functional reconstitution of a large class of transmembrane proteins and has a high electrical resistivity, we synthesized 18-octadecyl-1-thiahexa(ethylene oxide) [$HS(CH_2CH_2O)_6C_{18}H_{37}$, herein called THEO-$C_{18}$].

A hexa(ethylene oxide), HEO, segment in THEO-C_{18} between the alkane chain and the sulfur atom should be a useful moiety to accommodate extramembranous regions of proteins because poly(ethylene oxide), PEO, is highly water soluble. There have been several reports of other thiols with ethylene oxide (EO) spacer units conjugated to alkanes or lipids.[10,11,14,15] Lang et al. and Duschl et al.[11,14] described the synthesis of a series of thiolipids ($[R(EO)_xS]_2$, where R = dialkylglycerolphosphatidyl and $x = 1-3$) on which stable lipid bilayers formed. In another study, Williams et al.[10] showed that a mixed monolayer of $HO[EO]_3SH$ and the cholesterol-containing thiol [HS-$(EO)_3NHCO_2(C_{27}H_{44})$] formed a support layer for a bilayer membrane with phospholipids in the outer leaflet. More

* To whom correspondence should be addressed. John J. Kasianowicz, Ph.D., NIST, Biotechnology Division, ACSL 227/A251, Gaithersburg, MD 20899-8313. Phone: 301.975.5853. Fax: 301.330.3447. E-mail: john.kasianowicz@nist.gov.

† National Institute of Standards and Technology.

‡ The Texas A&M University System.

§ Vilnius University.

(1) Florin, E. L.; Gaub, H. E. *Biophys. J.* **1993**, *64*, 375.
(2) Seifert, K.; Fendler, K.; Bamberg, E. *Biophys. J.* **1993**, *64*, 384.
(3) Stelzle, M.; Wiessmuller, G.; Sackmann, E. *J. Phys. Chem.* **1993**, *97*, 2974.
(4) Plant, A. L. *Langmuir* **1993**, *9*, 2764.
(5) Plant, A. L.; Gueguetchkeri, M.; Yap, W. *Biophys. J.* **1994**, *67*, 1126.
(6) Plant, A. L.; Brigham-Burke, M.; O'Shannessy, D. *Anal. Biochem.* **1995**, *226*, 342.
(7) Meuse, C. W.; Niaura, G.; Lewis, M. L.; Plant, A. L. *Langmuir* **1998**, *14*, 1604.
(8) Meuse, C. W.; Kreuger, S.; Majkrzak, C. F.; Dura, J.; Fu, J.; Conner, J. T.; Plant, A. L. *Biophys. J.* **1998**, *74*, 1388.
(9) Bunjes, N.; Schmidt, E.; Jonczyk, A.; Rippmann, F.; Beyer, D.; Ringsdorf, H.; Graber, P.; Knoll, W.; Naumann, R. *Langmuir* **1997**, *13*, 68.
(10) Williams, L.; Evans, S.; Flynn, T.; Marsh, A.; Knowles, P.; Bushby, R.; Boden, N. *Langmuir* **1997**, *13*, 751 and all references therein.
(11) Lang, H.; Duschl, C.; Vogel, H. *Langmuir* **1994**, *10*, 197.
(12) Duschl, C.; Liley, M.; Corradin, G. *Biophys. J.* **1994**, *67*, 1229.
(13) Naumann, R.; Jonczyk, A.; Kopp, R.; van Esch, J.; Ringsdorf, H.; Knoll, W.; Graber, P. *Angew. Chem., Int. Ed. Engl.* **1995**, *34*, 2056.
(14) Duschl, C.; Liley, M.; Lang, H.; Ghandi, A.; Zakeeruddin, S.; Stahlberg, H.; Dubochet, J.; Nemetz, A.; Knoll, W.; Vogel, H. *Mater. Sci. Eng.* **1996**, *C4*, 7.
(15) Cornell, B. A.; Braach-Maksvytis, V. L. B.; King, L. G.; Osman, P. D. J.; Ragues, B.; Pace, R. J. *Nature* **1997**, *387*, 580 and supplemental information.

10.1021/la000690k Published 2000 by the American Chemical Society
Published on Web 12/02/2000

recently, Cornell and colleagues demonstrated that lipids and branched alkanes containing three or four EO units linked by diester groups permit the reconstitution of the gramicidin ion channel into tethered SBMs.[15,16]

THEO-C_{18} differs from the alkylthiols noted above because it has six consecutive EO groups and no non-EO moieties in the spacer region. Reflection absorption infrared spectroscopy measurements of THEO-C_{18} monolayers in air suggested that the monolayers were ordered and that the HEO spacer adopted a 7/2 helix oriented normal to the gold support surface.[17] However, that study did not determine whether this spacer could be hydrated after the complete assembly of a supported bilayer membrane.

We report here the electrical properties of monolayers of THEO-C_{18} and SBMs that consist of phospholipid on those monolayers, as determined by ac impedance spectroscopy and voltammetric methods. These measurements provide insight into the structure, stability, and ionic permeability of the monolayers and bilayers. We also show that the pore-forming protein αHL incorporates into these membranes to a certain degree. Interestingly, the results suggest that even in the presence of a pore-forming toxin the THEO segment is not well hydrated.

Experimental Methods

The synthesis of THEO-C_{18} was described previously.[17] Egg phosphatidylcholine (egg PC) was obtained from Avanti Polar Lipid (Alabaster, AL). Wild-type αHL was prepared as previously reported.[18] Silicon wafers (Si-Tech, Inc., Topsfield, MA, 100 orientation, 75 mm diameter, lot 11670) were cleaned for 30 min in potassium persulfate/sulfuric acid solution followed by rinses in deionized water and then methanol (reagent grade, J. T. Baker, Phillipsburg, NJ). The wafers were dried under a nitrogen stream. Gold (150 nm on a 2.5 nm thermally evaporated chromium adhesion layer) was sputter deposited onto the wafers in an Auto 306 system from Edwards High Vacuum International (West Sussex, U.K.). After the wafers were cooled to ambient temperature under vacuum, they were removed from the sputtering chamber and immediately immersed into a 0.001 mol/L solution of THEO-C_{18} or octadecanethiol ($C_{18}H_{37}SH$) [$C_{18}SH$] (Aldrich Chemical Co., Milwaukee, WI) in hexadecane (Aldrich). The wafers were kept in the solution for at least 16 h and were subsequently rinsed with hexanes (reagent grade, Mallinckrodt Baker, Paris, KY).

Entire wafers were assembled into an eight-cell Teflon electrochemical chamber. In each cell, 0.3 cm^2 of wafer was exposed to aqueous solution. Bilayers were formed on these areas by incubating with liposomes, as described below, for 1 h. Impedance measurements demonstrated that this incubation period was sufficient for bilayer formation.

Liposomes were prepared by evaporating $CHCl_3$ from 25 mg of egg PC with a nitrogen stream and vacuum-drying the lipid overnight. The lipid was then dissolved in 0.8 mL of *i*-propanol, and this was injected, while rapidly mixing, into 16.4 mL of buffer solution. The buffer solution used throughout this work contained 0.1 mol/L KH_2PO_4 and 0.001 M EDTA (ethylenediaminetetraacetic acid) with adjustment to pH 7 using KOH.

The effects of the pore-forming toxin *Staphylococcus aureus* αHL on the ac impedance and the permeability of the phospholipid/THEO-C_{18} SBMs to redox ions were determined after adding 43 μg of the protein (1.3×10^{-9} moles in 108 μL) to each electrochemical cell and diluting to a total volume of 0.4 mL with buffer. The toxin was also added to phospholipid/$C_{18}SH$ SBMs by adding 20 μg of αHL (0.6×10^{-9} moles in 50 μL) to each well and diluting to a total volume of 0.2 mL. As a control, adjacent cells were filled with the same buffer without αHL. The cells containing SBMs with or without the pore-forming protein were incubated for more than 12−18 h.[19] After incubation, the cells were rinsed with 0.1 mol/L KH_2PO_4−1 mol/L KCl−0.001 mol/L EDTA, pH 7.0, before the impedance measurements were made.

We also reconstituted αHL into the SBMs by exposing the THEO-C_{18} monolayer on gold to lipid vesicles that were preincubated with αHL. The lipid vesicle preparation was diluted 50/50 (v/v) with an aqueous solution of αHL to give a lipid-to-protein molar ratio of 144:1. The protein was allowed to incorporate into the vesicles overnight at 4 °C. These vesicles were subsequently incubated with the monolayers for 1 h after they had equilibrated to room temperature. As a control, vesicles that were not exposed to αHL were added to monolayers in adjacent cells on the same gold-coated wafer. The impedance measurements were made in the presence of vesicles. The excess vesicles were flushed from the bilayers before square wave voltammetry measurements were made in the presence of ferricyanide.

Electrochemical measurements were made using a BAS 100 B/W electrochemical analyzer in the three-electrode configuration (Bioanalytical Systems, West Lafayette, IN). The working and counter electrodes were the gold surface and a platinum wire, respectively. The reference electrodes were Ag/AgCl (Bioanalytical Systems and WPI, Sarasota, FL) filled with 3 M KCl solution. In this work, all potentials were reported with respect to this reference electrode. The fitting of the ac impedance spectra to equivalent circuit models was performed with the ZView 2.0 software (Scribner Associates, Southern Pines, NC).

Impedance measurements were made at 0 mV versus the reference electrode with a 5 mV ac signal. The frequency was varied from 1 to 1000 Hz. Cyclic voltammetry scans were carried out at the scan rate of 50 mV/s. Square wave voltammetry was typically performed between 400 and −400 mV versus the reference electrode with steps of 4 mV, a square wave amplitude of 25 mV, and a frequency of 15 Hz. All chemicals were reagent grade. Aqueous solutions were prepared in deionized water from a Barnstead Nanopure II system (Barnstead, Dubuque, IA).

Results and Discussion

Monolayer and Bilayer Impedance Measurements, Equivalent Circuit Models. The electrical properties of THEO-C_{18} monolayers and phospholipid/THEO-C_{18} SBMs were characterized using ac impedance spectroscopy. The total impedance, $Z = Z_{real} + jZ_{imag}$ (where Z_{real} and Z_{imag} are the real and imaginary components of the impedance, respectively, and $j = (-1)^{1/2}$), was measured between 1 and 1000 Hz. Figures 1 and 2 illustrate the impedance data obtained with THEO-C_{18} monolayers and phospholipid/THEO-C_{18} bilayers, respectively. As expected, the impedance magnitude of the monolayer is less than that of the bilayer (Figures 1A and 2A). The phase angles, $\varphi = \tan^{-1}(Z_{imag}/Z_{real})$, of both surfaces are slightly less than −90° over most of the entire frequency range (Figures 1B and 2B), which suggests that the capacitive reactance of the thin films dominates the impedance. In addition, the phase angle tends to decrease with decreasing frequency.

Plots of the impedance data in the form of the imaginary versus the real components of the complex admittance (Im Y/ω vs Re Y/ω, where $Y = Z^{-1}$) illustrate the impedance behavior for SAMs and SBMs containing THEO-C_{18} (Figures 1C and 2C). For both films, Im Y/ω increases with increasing Re Y/ω.

In the absence of electron transfer, several simple equivalent circuit schemes are used to model the impedance spectra of the SAMs and SBMs.[4,20] A widely accepted model is a series RC circuit, where R represents the solution resistance and C represents the monolayer or bilayer

(16) Raguse, B.; Braach-Maksvytis, V.; Cornell, B. A.; King, L. G.; Osman, P. D. J.; Pace, R. J.; Wieczorek, L. *Langmuir* **1998**, *14*, 648.
(17) Vanderah, D. J.; Meuse, C. W.; Silin, V. I.; Plant, A. L. *Langmuir* **1998**, *14*, 6916.
(18) Cheley, S.; Malghani, M. S.; Song, L. S.; Hobaugh, M.; Gouaux, J. E.; Yang, J.; Bayley, H. *Protein Eng.* **1997**, *10*, 1433.
(19) Fang, Y.; Cheley, S.; Bayley, H.; Yang, J. *Biochemistry* **1997**, *36*, 9518.
(20) Diao, P.; Jiang, D.; Cui, X.; Tong, R.; Zhong, B. *J. Electroanal. Chem.* **1999**, *464*, 61.

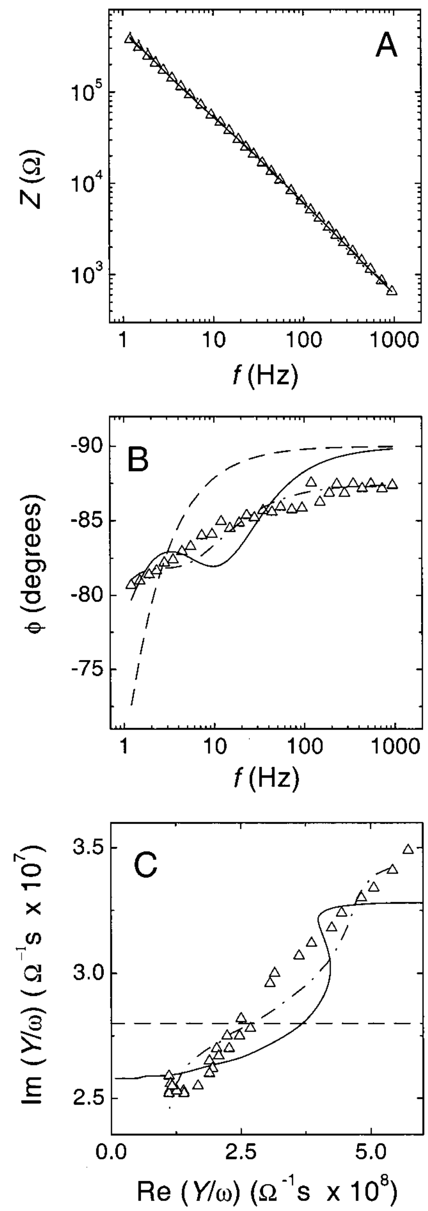

Figure 1. Typical ac impedance of THEO-C_{18} self-assembled monolayers: (A) impedance magnitude vs frequency, (B) impedance phase angle vs frequency, and (C) admittance plot of Re Y/ω vs Im Y/ω. The dashed, solid, and dotted−dashed lines are the results of least-squares fits of three equivalent circuit models (a parallel RC circuit, two parallel RC circuits in series, and two parallel R-CPE circuits in series, respectively; see Figure 3) to the data. The solutions contained 0.1 mol/L KH_2PO_4 and 1 mol/L KCl, pH 7.0, under nitrogen purge. The measurements were performed at 0 V dc vs Ag/AgCl, 3 M KCl reference electrode.

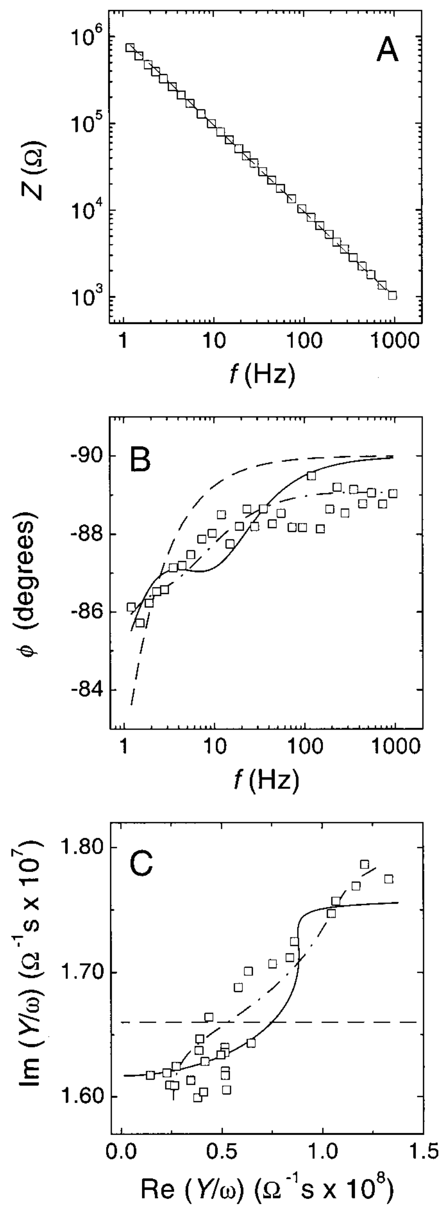

Figure 2. Impedance data for THEO-C_{18}/egg PC supported bilayer membranes: (A) impedance magnitude vs frequency, (B) impedance phase angle vs frequency, and (C) admittance plot of Re Y/ω vs Im Y/ω. See the Figure 1 legend for the description of the experimental conditions and data fitting procedure.

capacitance. In the presence of the redox species and/or in the presence of the pinholes (i.e., bare patches that are not covered by alkanethiol) or immobilized ionic channels, a parallel RC equivalent scheme is assumed.[5,15,16] Occasionally, the models include constant phase elements (CPEs), instead of pure capacitances,[21] which reflect the deviation of the electrode impedance from ideal capacitive behavior.[22] In the presence of a CPE, the electrode impedance has a power law frequency dependence $Z = (1/\sigma)^{\alpha}(j\omega)^{-\alpha}$ where ω is the cyclic frequency, σ is the CPE constant, and α is the CPE exponent ($0.5 < \alpha < 1$). CPE behavior is usually observed in systems with various kinds of heterogeneity, for example, geometric (roughness), energetic (distributed time constants of slowly relaxing processes), or physical (different crystallographic planes on the surface).[22]

To interpret the impedance data, we considered three different equivalent circuit models (Figure 3): a parallel RC circuit (model a), two parallel RC circuits in series (model b), and two parallel R-CPE circuits in series (model c). The admittance plots for these circuits are shown in Figures 1C and 2C. For a parallel RC circuit, the imaginary component of the Y/ω is independent of frequency and of Re Y/ω (dashed line) and therefore does not describe the impedance data for THEO-C_{18} monolayers and phospholipid/THEO-C_{18} SBMs. Unlike SAMs and SBMs made with alkanethiol monolayers, the THEO-alkane films used here have two ponderable and distinct dielectric regions. Specifically, the HEO and alkane segments have bulk

(21) Lindholm-Sethson, B. *Langmuir* **1996**, *12*, 3305.
(22) Pajkossy, T. *J. Electroanal. Chem.* **1994**, *364*, 111.

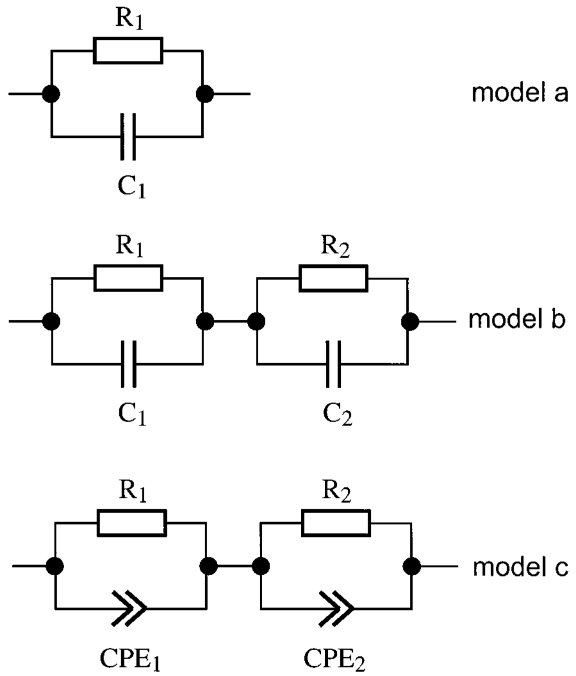

Figure 3. Equivalent circuit models used to describe the impedance of self-assembled monolayers and supported bilayer membranes used in this study.

dielectric permittivities of ∼20 (see ref 23) and 2.1 (see ref 24), respectively. Therefore, one might expect the two parallel RC circuit or the two parallel R-CPE circuit impedance responses to provide a better fit to the SAM and SBM impedance data than would a single parallel RC model. They do (Figures 1C and 2C, Table 1A,B). The better fit of the R-CPE model to the data, as judged by the χ^2 function,[25] suggests that the thiol layer may be slightly disordered.

The fit parameters for the THEO-C_{18} SAMs in Table 1A show that one parallel R-CPE circuit contains a high resistance and low effective capacitance ($R_1 = 4.8$ MΩ, $\sigma_1 = 0.366$ μF) whereas the other R-CPE circuit has a lower resistance and higher effective capacitance ($R_2 = 29$ kΩ, $\sigma_2 = 2.2$ μF). Unfortunately, the impedance data do not determine which of the R−σ value pairs correspond to the THEO and C_{18} alkane layers. However, we can make a preliminary assignment based on other experimental information. First, adding a phospholipid layer atop the THEO-C_{18} monolayer increases the value of R_1 3.5-fold and decreases σ_1 nearly 2-fold (Table 1A,B). Both results are consistent with assigning the R_1−CPE_1 equivalent circuit to the alkane portion of the THEO-C_{18} monolayer. Second, the value of the CPE exponent α_1 is ∼1 (i.e., the data are only slightly better described by the two R-CPE model compared to the two RC model). Thus, we assume that $\sigma_1 \approx C_{ALK}$, where C_{ALK} is the capacitance of the alkane portion of the monolayer. The specific capacitance for this segment is 0.366 μF/0.31 cm^2 = 1.18 μF cm^{-2}. This is in good agreement with the specific capacitance of a C_{18}SH monolayer (1 μF/cm^2).[26] The slightly higher specific capacitance might be due to a slightly greater actual surface area, caused by surface roughness, compared to the geometric area of the electrode used in our calculations.

(23) Fanggao, C.; Saunders, G. A.; Lambson, E. F.; Hampton, R. N.; Carini, G.; DiMarco, G. *J. Polym. Sci., Part B* **1996**, *34*, 425.
(24) Dilger, J. A.; McLaughlin, S. G. A.; McIntosh, T. J.; Simon, S. A. *Science* **1979**, *206*, 1196.
(25) Macdonald, J. R. *Complex Nonlinear Least Squares Immitance Fitting Program. LEVM manual*, version 7.11.
(26) Porter, M. D.; Bright, T. B.; Allara, D. L; Chidsey, C. E. D. *J. Am. Chem. Soc.* **1987**, *109*, 3559.

Table 1

A. Impedance Analysis of THEO-C_{18} Monolayers

impedance parameter	model a	model b	model c
R_1, MΩ	1.51 ± 0.24	2.56 ± 0.30	4.8 ± 0.5
C_1, μF	0.28 ± 0.04	0.332 ± 0.004	
R_2, MΩ		0.011 ± 0.001	0.029 ± 0.005
C_2, μF		1.16 ± 0.05	
σ_1, μF			0.366 ± 0.003
α_1			0.98 ± 0.00
σ_2, μF			2.20 ± 0.11
α_2			0.94 ± 0.01
$\chi^2 \times 10^3$	586	15.8	1.71

B. Impedance Analysis of THEO-C_{18}/Egg PC Supported Bilayer Membranes

impedance parameter	model a	model b	model c
R_1, MΩ	7.15 ± 1.10	11.1 ± 1.30	16.8 ± 4.9
C_1, μF	0.166 ± 0.01	0.18 ± 0.01	
R_2, MΩ		8.08 ± 1.27	24.3 ± 20.5
C_2, μF		1.98 ± 0.12	
σ_1, μF			0.181 ± 0.01
α_1			0.99 ± 0.02
σ_2, μF			2.7 ± 1.1
α_2			0.91 ± 0.07
$\chi^2 \times 10^3$	201	15.8	1.85

Even with the addition of a phospholipid layer, the CPE exponent α_1 is still nearly equal to 1 (Table 1B). Thus, we assume that $\sigma_1 \approx C_{TOT}$, where C_{TOT} corresponds to the capacitance of the alkane layer formed by the methyl groups of both THEO-C_{18} and the lipid hydrocarbon moiety:

$$1/C_{TOT} = 1/C_{ALK} + 1/C_{PL} \qquad (1)$$

where C_{ALK} and C_{PL} are the capacitances of the THEO-C_{18} alkane and the phospholipid monolayers. The latter is estimated from $C_{PL} = \epsilon_0 \epsilon_{PL} S/d_{PL}$, where ϵ_0 is the vacuum permittivity, ϵ is the lipid's dielectric constant ($\epsilon_{PL} = 2.1$, ref 24), S is the surface area, and d is the lipid monolayer thickness ($d_{PL} = 1.22$ nm and is assumed to be half the thickness of a solvent-free egg PC bilayer[27]). A spectroscopic study by Meuse et al.[8] suggests that only subtle structural changes of long-chain alkanethiol monolayers occur after a lipid monolayer is adsorbed to a THEO-C_{18} SAM. We therefore assume that the impedance properties of the alkanethiol are the same for THEO-C_{18} SAMs with or without a phospholipid monolayer atop them.[8] Therefore, using $C_{PL} = 0.46$ μF and $C_{ALK} = 0.37$ μF (σ_1, Table 1A), $C_{TOT} = 0.21$ μF. This is only 10% greater than the value of $\sigma_1 = 0.181$ μF obtained using the CPE fit values (Table 1B). We therefore conclude that the R_1-CPE_1 parallel equivalent circuit adequately represents the physical properties of the alkane segments of both THEO-C_{18} SAMs and the phospholipid/THEO-C_{18} SBMs.

The capacitance of the HEO segment, $C_{HEO} = 3.31$ μF, is estimated using $\epsilon_{HEO} = 20$, which corresponds to the dielectric constant for bulk unhydrated PEO,[23] and $d_{HEO} = 1.66$ nm, which is the thickness of HEO calculated from the crystallographic data of PEO assuming the HEO adopts an ordered 7/2 helical structure of the THEO segment.[17] This capacitance value is significantly greater than the values of σ_2 obtained for the SAMs and SBMs (2.20 and 2.7 μF, respectively). However, it is

(27) Fettiplace, R.; Andrews, D. M.; Haydon, D. A. *J. Membr. Biol.* **1971**, *5*, 277.

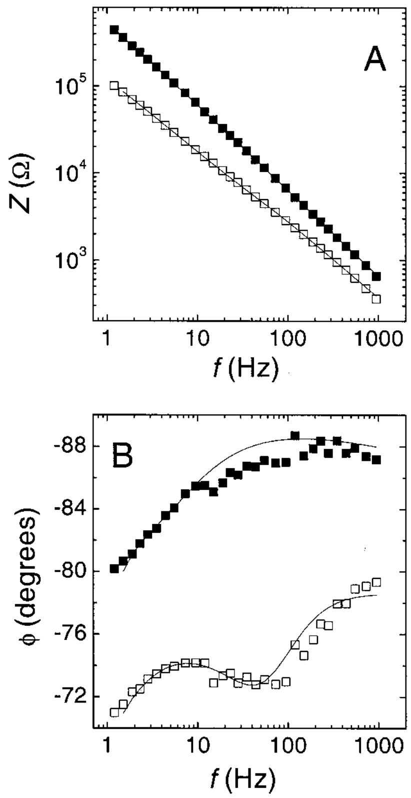

Figure 4. Time course of changes in impedance magnitude spectra at 600 mV dc applied potential vs Ag/AgCl for a THEO-C_{18} monolayer. The 1st impedance spectrum is represented by filled squares, and the 15th impedance spectrum is represented by open squares. The time between spectra is ~60 min. The solution contained 0.1 mol/L KH_2PO_4 and 1 mol/L KCl, pH 7.0, and was kept under nitrogen purge.

difficult to obtain a precise evaluation of the R_2-CPE_2 circuit parameters because the impedance of the HEO segment is much less than that of the THEO-C_{18} alkane segment. Therefore, small errors in the experimentally measured impedance cause a greater uncertainty in the calculated parameters which we assign to the HEO fragment (Table 1A,B). Nevertheless, the assignment of the R_1-CPE_1 and R_2-CPE_2 fit values to the alkane and HEO segments of THEO-C_{18} is reasonable because the formation of the phospholipid layer on the top of the THEO-C_{18} monolayer strongly affects the parameters of the R_1-CPE_1 circuit (the alkane portion), whereas the values of R_2-CPE_2 circuit (HEO segment) remain constant within the experimental uncertainty.

Monolayer and Bilayer Stability at Varying dc Potentials. Anticipating future applications for supported membranes that require working potentials other than 0 mV versus Ag/AgCl, we measured the stability of the monolayers and bilayers at a number of dc potentials through repeated ac impedance measurements. Figure 4 illustrates the decrease in impedance magnitude of a THEO-C_{18} monolayer (at 600 mV vs Ag/AgCl) that occurred after the acquisition of 15 consecutive spectra (during which the dc potential was applied for a total of 60 min). The magnitude of the impedance change is smaller at −600 mV applied dc potential (data not shown). Potentials between ±400 mV cause virtually no change in the impedance (data not shown). Data were taken on different monolayers at each potential. The initial impedance spectra of the SAMs at 0 mV versus Ag/AgCl were similar. For monolayers, the greater the absolute value of the applied potential, the greater the decrease in the impedance. The same was true for the bilayers. However,

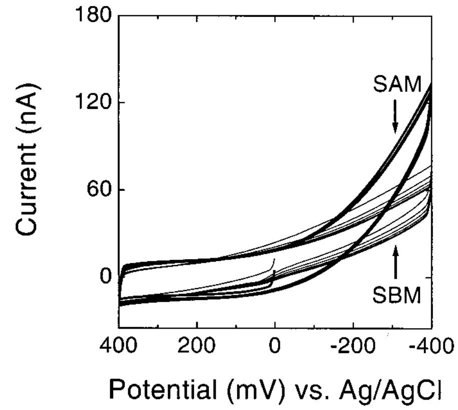

Figure 5. Cyclic voltammograms of THEO-C_{18} monolayers (SAM) and THEO-C_{18}/egg PC bilayers (SBM) in the presence of 10^{-3} mol/L ferricyanide. The results are the average values for seven different surfaces.

for SBMs the maximum change in the impedance is about 5-fold less than that for monolayers. The added stability might be due to either a decrease in the potential drop across the monolayer when a bilayer is present or a decrease in the electrolyte's partition coefficient into the bilayer compared to that of the monolayer or both.

Impedance analysis shows that the R-CPE equivalent circuit (Figure 3, model c) is still the best fitting model after the monolayers were subjected to a large dc polarization of +0.6 V. The results suggest that the qualitative changes of the curves in Figure 4 are caused by changes to the alkane segment of the monolayer. For example, for the experimental data shown in Figure 4, we observed a 5-fold increase of σ_1 and a 3-fold decrease of the resistance R_1 upon polarization of the monolayer at $E = +0.6$ V for 60 min. In addition, the CPE_1 exponent α_1 decreased from 1.0 to 0.86, suggesting that the large dc potential caused an increase in the monolayer's disorder. Thus, polarization at high potentials may cause partial destruction or desorption of SAMs composed of THEO-C_{18}. However, dc potentials with absolute magnitudes less than 400 mV versus Ag/AgCl, at least for periods shorter than 60 min, had little effect on the impedance of the supported monolayers or supported bilayers and, by inference, on the supported membrane's structure.

Another measure of the THEO-C_{18} monolayer's structural order and stability and the extent to which it covers the gold electrode is the SBM's ability to block ferricyanide oxidation/reduction during repeated cyclic voltammetry. The degree of ion blocking indicates the fraction of the monolayer's area that can be attributed to pinholes or other defects. Microscopic holes through a thin film that persist to the working electrode's gold surface are assumed to exist if there are redox current peaks or plateaus in voltammograms at low overpotentials.[28] Typical THEO-C_{18} monolayer and phospholipid/THEO-C_{18} bilayer cyclic voltammograms (Figure 5) show that the monolayers are virtually free of pinholes (as evidenced by the lack of current peaks or plateaus in the region of 265 mV, the formal potential for ferricyanide under these conditions). The blocking of the gold surface by THEO-C_{18}, relative to bare gold, is virtually complete, >99% as calculated according to Chen et al.[29] at the reduction and oxidation

(28) Finklea, H. O. Electrochemistry of Organized Monolayers of Thiols and Related Molecules on Electrodes. In *Electroanalytical Chemistry*; Bard, A. J., Rubenstein, I., Eds.; Marcel Dekker: New York, 1996; Vol. 19, pp 180−181.

(29) Chen, C.; Hutchison, J. E.; Postlethwaite, T. A.; Richardson, J. N.; Murray, R. W. *Langmuir* **1994**, *10*, 3332.

peak potentials on bare gold of 236 and 294 mV, respectively (thick line, Figure 5). The blocking values are calculated using cyclic voltammograms from +400 to −100 mV with corresponding voltammograms for bare gold by dividing the current for the monolayers at the peak potentials by that of a bare gold surface (data not shown). In addition, the voltammograms for the bilayer (thin line, Figure 4) demonstrate that compared to the monolayer alone the additional phospholipid layer increases the thin film's effectiveness in blocking the ferricyanide electrochemical reaction.

Effect of the Pore-Forming Protein αHL on SBM Impedance. One of the goals of this study was to determine whether integral membrane proteins can functionally reconstitute into supported phospholipid/THEO-C_{18} bilayers. To address this, we examined the effect of the pore-forming protein α-hemolysin (αHL)[30,31] on the conducting properties of SBMs. Wild-type αHL reconstituted into planar bilayer membranes has been used to measure the concentration of different analytes (e.g., protons,[32,33] deuterium ions,[33] and single-stranded polynucleotides[34]). Genetically engineered versions of αHL have been used to quantitate the concentration and type of heavy metal divalent cations in solution.[35−38] Hence, reconstitution of αHL into SBMs may prove useful in sensing applications.

The results of ac impedance measurements performed at 0 mV dc potential versus Ag/AgCl on individual SBMs incubated for more than 12 h with the protein are shown in Figure 6A−C. The SBMs were found to be stable over the total time of the experiment. The data in Figure 6A,B demonstrate that, as expected, αHL decreases the SBM impedance magnitude. However, the effect of the αHL on the SBMs is bimodal. In some experiments, αHL added to the bulk aqueous phase causes a decrease in the impedance magnitude over the entire frequency range (Figure 6A) and no change in phase angle (data not shown). In the latter case, fitting the data to the R-CPE equivalent circuit (Figure 3, model c) shows that the magnitude decreases because the CPE_1 coefficient, σ_1, increases ca. 1.5-fold. This suggests that the capacitance of the alkane segment increases after αHL interacts with the SBM. No significant changes were observed in the HEO layer's fit parameters. This suggests that the protein is penetrating only to the outermost layer of the SBM.

In another group of experiments, the decrease in the impedance magnitude that occurred after incubation of the SBMs with αHL depended on the frequency (Figure 6B). At low frequencies, the decrease was much greater than that at higher frequencies. In addition, a deviation from linearity of log Z versus $\log_{10} f$ (Figure 6B) is evident. The phase angle of SBMs incubated with αHL (Figure 6C) exhibits a minimum near $f \sim 100$ Hz. The depth of the minimum was poorly reproducible (compare the results of two independent experiments, open circles vs open squares). Nevertheless, the R-CPE equivalent circuit (Figure 3, model c) gives the best fits to the data in Figure 6 (Table 2).

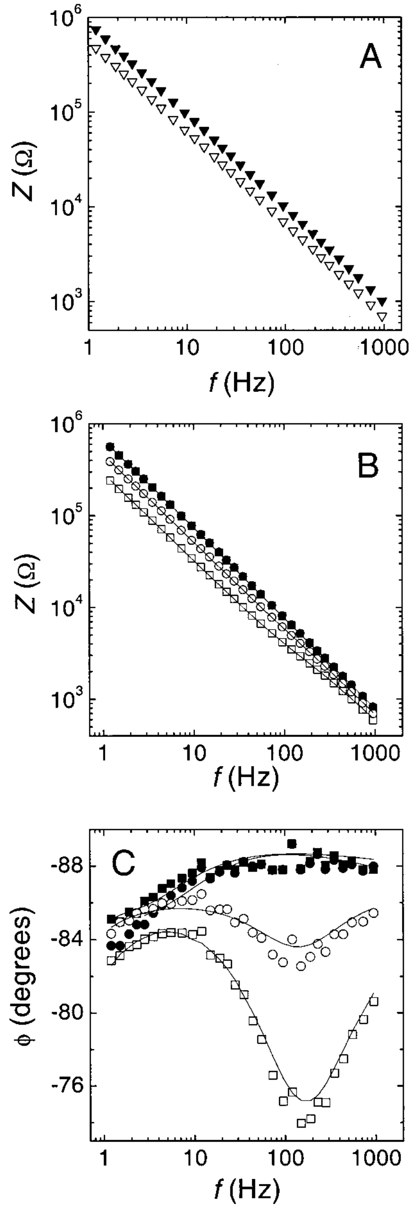

Figure 6. Effect of αHL on the ac impedance of THEO-C_{18}/egg PC SBMs. The closed and open symbols represent the values of the impedance parameters before and after incubation, respectively. (A) The impedance magnitude spectra for which no change in the impedance phase angle occurs after incubation with αHL. (B) The extremes in the change of the bilayer impedance magnitude for two bilayers for which there were significant changes in the phase angle. (C) The frequency dependence of the impedance phase angle. The solid lines in (B) and (C) are least-squares fits to the double R-CPE equivalent circuit model c (Figure 3). The solution bathing the SBMs is 0.1 mol/L KH_2PO_4 and 1 mol/L KCl, pH 7.0, under nitrogen purge.

We emphasize that in the second group of experiments, two parameters change upon incubation of the SBMs with αHL. First, the resistance R_2, that we assigned to the HEO segment, decreased sharply, typically by ∼2 orders of magnitude (Table 2). Second, the capacitance of the alkane segment of the bilayer increased, with an accompanying slight decrease of the CPE exponent value. The capacitance increase might be caused by a

(30) Bhakdi, S.; Tranum-Jensen, J. *Microbiol. Rev.* **1991**, *55*, 733.
(31) Gouaux, J. E. et al.; Bayley, H. *Proc. Natl. Acad. Sci. U.S.A.* **1994**, *91*, 12828.
(32) Bezrukov, S. M.; Kasianowicz, J. J. *Phys. Rev. Lett.* **1993**, *70*, 2352.
(33) Kasianowicz, J. J.; Bezrukov, S. M. *Biophys. J.* **1995**, *69*, 94.
(34) Kasianowicz, J. J.; Brandin, E.; Branton, D.; Deamer, D. W. *Proc. Natl. Acad. Sci. U.S.A.* **1996**, *93*, 13770. Henrickson, S. E.; Misakian, M.; Robertson, B.; Kasianowicz, J. J. *Phys. Rev. Lett.* **2000**, *85*, 3057.
(35) Walker, B.; Kasianowicz, J.; Krishnasastry, M.; Bayley, H. *Protein Eng.* **1994**, *7*, 655. Kasianowicz, J.; Walker, B.; Krishnasastry, M.; Bayley, H. *MRS Symp.* **1994**, *330*, 217.
(36) Braha, O.; Walker, B.; Cheley, S.; Kasianowicz, J. J.; Song, L.; Gouaux, J. E.; Bayley, H. *Chem. Biol.* **1997**, *4*, 497.
(37) Kasianowicz, J. J.; Burden, D. L.; Han, L.; Cheley, S.; Bayley, H. *Biophys. J.* **1999**, *76*, 837.
(38) Miller, C.; Cuendet, P.; Gratzel, M. *J. Electroanal. Chem.* **1990**, *278*, 175.

Table 2. Impedance Analysis of THEO-C_{18}/Egg PC Supported Bilayer Membranes in the Presence of αHL Incorporation[a]

impedance parameter	open circles, Figure 6B,C	open squares, Figure 6B,C
R_1, MΩ	14.5 ± 4.0	4.33 ± 0.67
σ_1, μF	0.369 ± 0.03	0.592 ± 0.056
α_1	0.96 ± 0.00	0.96 ± 0.00
R_2, kΩ	370 ± 81	929 ± 58
σ_2, μF	2.76 ± 0.84	1.378 ± 0.158
α_2	0.99 ± 0.05	0.93 ± 0.02
$\chi^2 \times 10^3$	0.96	0.79

[a] An impedance model of two parallel R-CPE circuits in series is used (Figure 3, model c) to fit the data in Figure 6.

decrease in the hydrocarbon layer thickness or an increase in this segment's dielectric constant. The latter might be caused by the greater dielectric constant of the αHL itself or by the water in pores formed by αHL. The putative changes to the HEO and hydrocarbon segments suggests that αHL partially or wholly penetrates the SBMs.

The penetration of the water- and electrolyte-filled αHL pores into the SBM should decrease the resistance of the alkane layer (R_1, Figure 3, model c). In some cases, that did occur. Curiously, in other occasions we observed the opposite effect. However, the poor reproducibility could be related to the significant relative uncertainty of R_1. Indeed, even at $f = 1$ Hz (the lowest frequency employed in the present work) the conductivity of CPE_1 is ~35 times greater than that of the R_1 element (fourth column of Table 2). Thus, R_1 represents ~3% of the total impedance of the alkane segment of SBM.

We do not completely understand the bimodal changes observed in the electrical parameters of these SBMs upon incorporation of αHL. It is conceivable that the degree of molecular order in the SBM may vary from sample to sample under identical conditions, as was observed by Miller et al.[38] We hypothesize that the degree of SBM order, which may depend on a number of factors as was shown for SAMs of related amphiphiles,[39] will affect the depth of penetration by αHL. For samples in which a highly ordered bilayer is formed, the αHL molecules may not be able to penetrate through the alkane segment of the SBM. In this case, one would observe only a slight decrease of the impedance magnitude (e.g., Figure 6A). However, for SBMs that contain less order, deeper penetration of αHL into the SBM might occur. In this case, one would expect the changes, both in the outermost and underlying HEO segment of the SBM, that are observed in the present work (Table 2).

Effect of αHL on SBM Permeability to Ferricyanide. The αHL channel has a diameter of ca. 1.5–2 nm.[40–42] It follows that it should increase the permeability of SBMs to ferricyanide. The in-phase component of square wave voltammetry for SBMs in the absence (Figure 7A, filled circles) and presence (Figure 7A, open circles) of αHL was determined. Adding αHL directly to the solution bathing the SBM (method 1, see above) causes a marked increase in the reductive current as the potential is stepped from +400 mV to less positive potentials. Essentially the same result is obtained when we reconstitute αHL into phospholipid vesicles and adsorb these vesicles onto a THEO-C_{18} SAM (Figure 7B). Thus, αHL increases the permeability of the THEO-C_{18}/egg PC SBMs to ferricyanide ions.

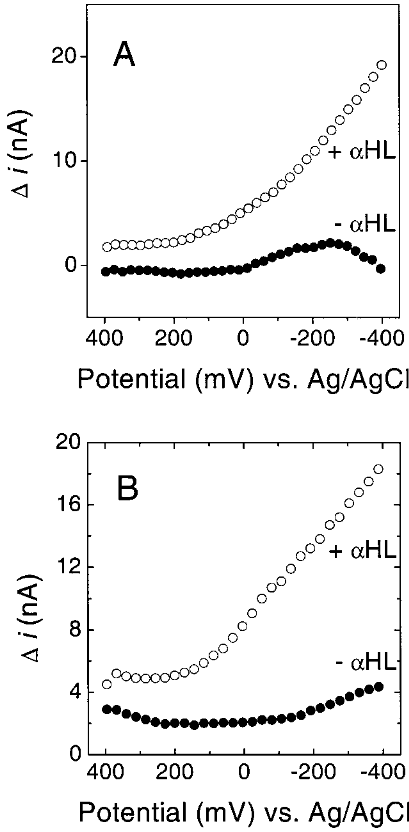

Figure 7. Square wave voltammograms for THEO-C_{18}/egg PC bilayers in the presence (open circles) and absence (filled circles) of αHL. The current is relative to the original. (A) αHL is directly added to the bathing solution (αHL reconstitution method 1). (B) αHL is added to the egg PC vesicles which are subsequently fused to THEO-C_{18} SAMs (αHL reconstitution method 2). The solution contains 0.1 mol/L KH_2PO_4 and 1 mol/L KCl, pH 7.0, and 10^{-3} mol/L ferricyanide under nitrogen purge.

Effect of the HEO Segment on αHL Reconstitution. To determine the influence of the HEO region on the reconstitution of αHL into SBMs, we also measured the impedance of bilayers composed of C_{18}SH/egg PC. Unlike THEO-C_{18}/egg PC SBMs doped with αHL, C_{18}SH/egg PC SBMs do not consistently show ferricyanide reduction currents (measured using square wave voltammetry) at negative potentials in the presence of αHL (data not shown). This suggests that in the C_{18}SH/egg PC bilayers αHL does not provide a continuous pathway for the redox species to migrate from the aqueous solution to the gold electrode. In unsupported bilayer membranes, the αHL channel extends past both membrane surfaces.[37,41] It is likely that the channel does not properly form if there is insufficient space available for the extramembranous segments of the protein.

A single series RC circuit adequately describes the impedance data for C_{18}SH/egg PC SBMs in the absence of αHL (Figure 8, filled squares). When these SBMs are doped with αHL (Figure 8, open squares), the phase angle varies nonmonotonically with frequency. In this case, at least two parallel RC or two R-CPE circuits in series (or one parallel RC circuit in series with one R-CPE circuit) are needed to describe the impedance magnitude, Z, and phase angle, ϕ, (Figure 8, open squares). The best least-squares fit is obtained using the double R-CPE model (Figure 3, model c). However, the frequency dispersion

(39) Harder, P.; Grunze, M.; Dahint, R.; Whitesides, G. M.; Laibinis, P. E. *J. Phys. Chem. B* **1998**, *102*, 426.
(40) Bezrukov, S. M.; Vodyanoy, I.; Brutyan, R. A.; Kasianowicz, J. J. *Macromolecules* **1996**, *29*, 8517.
(41) Song, L.; Hobaugh, M. R.; Shustak, C.; Cheley, S.; Bayley, H.; Gouaux, J. E. *Science* **1996**, *274*, 1859.
(42) Bezrukov, S. M.; Kasianowicz, J. J. *Eur. Biophys. J.* **1997**, *6*, 471.

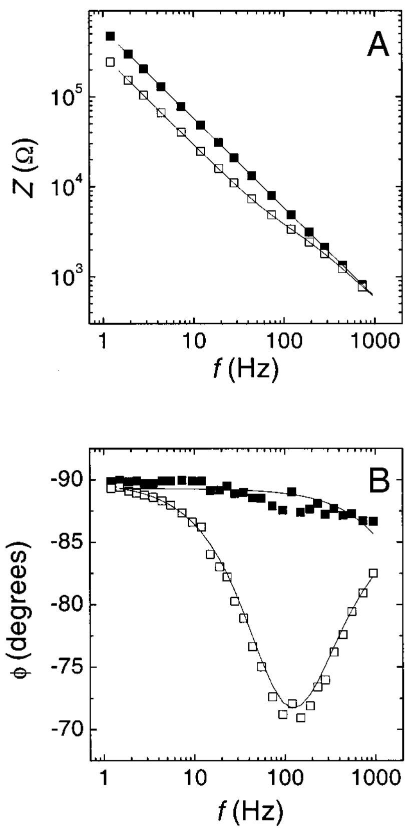

Figure 8. Effect of αHL incorporation on the ac impedance of $C_{18}SH$/egg PC supported bilayers. The frequency dependence of (A) the impedance magnitude and (B) the impedance phase angle. The closed and open symbols represent the bilayers before and after incubation with αHL, respectively. The solution contains 0.1 mol/L KH_2PO_4 and 1 mol/L KCl, pH 7.0, under nitrogen purge.

analysis shows that the impedance of R_2 is much greater than that of C_2. Thus, the equivalent circuit model can be simplified to a pure capacitance C_2 in series with a parallel R_1-CPE_1 circuit.[15] It is conceivable that a high degree of "crystallinity" of the $C_{18}SH$ layer does not permit the formation of fully functional channels as we suggested above to describe the voltammetry measurements on these surfaces. In that case, the segment of the bilayer closest to the bulk aqueous phase is penetrated by electrolyte-filled pores and is well characterized by a parallel RC circuit. The alkane segment furthest from the bulk aqueous phase is apparently not fully penetrated by the ion channel.

There have been several studies, including this report, on reconstituting pore-forming proteins into SBMs.[15,43−45] Although these molecules seem to function as pores in SBMs, it is yet to be determined whether they function in the same manner as they do in planar bilayers. This would be more conclusively established by measurements on single channels in SBMs.

Conclusions

In this study, we have taken the initial step toward incorporating αHL, a transmembrane protein with a known crystal structure, into supported bilayer membranes with properties that are defined by electrochemical and impedance measurements. We established the equivalent electrical circuit that reflects the two discrete dielectric regions (HEO and alkane layers) of THEO-C_{18} SAMs and of SBMs comprised of THEO-C_{18}/egg PC.

The presence of αHL in the SBMs is demonstrated using electrochemical measurements. Specifically, for THEO-C_{18}/egg PC SBMs, αHL generally causes a decrease in the impedance magnitude and an increase in ferricyanide Faradaic current. The results suggest that αHL at least partially reconstitutes in these SBMs. In contrast, although the low-frequency impedance of $C_{18}SH$/egg PC SBMs also decreases in the presence of αHL, electrochemical measurements on SBMs without HEO suggest that αHL does not completely penetrate the entire hydrocarbon segment of the SBM. Thus, the HEO spacer adjacent to the gold electrode surface apparently increases the ability of αHL to fully penetrate the alkane region of the SBM.

Acknowledgment. This work was supported in part by the NIST Advanced Technology Program (J.J.K.).

LA000690K

(43) Vogel, H. *Angew. Chem., Int. Ed.* **1999**, *38*, 389.
(44) Sackmann, E. *Langmuir* **1998**, *14*, 3118.
(45) Sackmann, E.; Tanaka, M. *Trends Biotechnol.* **2000**, *18*, 58.